Physical properties and electronic evolution of $Sr_2FeMo_{1-x}Nb_xO_6$ $(0 \leq x \leq 1)$

B.-G. Park, Y.-H. Jeong, and J.-H. Park*
Department of Physics, Pohang University of Science and Technology, Pohang 790-784, Korea

J. H. Song
Department of Physics, Chungnam National University, Daejeon 305-764, Korea

J.-Y. Kim
Pohang Accelerator Laboratory, Pohang University of Science and Technology, Pohang 790-784, Korea

H.-J. Noh
Department of Physics, Chonnam National University, Gwangju 500-757, Korea

H.-J. Lin and C. T. Chen
National Synchrotron Radiation Research Center, Hsinchu, 30076, Taiwan
(Received 24 April 2008; revised manuscript received 14 August 2008; published 7 January 2009)

We investigated magnetic and electronic properties of double perovskites $Sr_2FeMo_{1-x}Nb_xO_6$ $(0 \leq x \leq 1)$. As Nb substitution x increases, the system gradually loses all ferromagnetic metallic characters such as the ordered magnetic moment, the magnetic transition temperature T_C, the degree of cation-site ordering, and the metallic conductivity. For $x > 0.7$, the ferromagnetic characters disappear. The electronic structure was also investigated to explore its correlation with the physical properties by using the soft x-ray absorption spectroscopy at Fe $L_{2,3}$, Mo $M_{2,3}$, and O K edges. The Fe state, which is an Fe^{2+}-Fe^{3+} mixed valent state close to $Fe^{2.5+}$ in average at Sr_2FeMoO_6 $(x=0)$, becomes gradually transformed to be an Fe^{3+} monovalent state at Sr_2FeNbO_6 $(x=1)$ with the Nb substitution. The Mo valence state, approximately $Mo^{5.5+}$ $(4d^{0.5})$, does not show any considerable change for $0 \leq x < 1$. The replacement of Mo with Nb^{5+} $(4d^0)$ reduces the density of states at Fermi level, which corresponds to the Mo 4d-Fe 3d strongly mixed states, and cause the increase in resistivity. These results show that the loss of the ferromagnetic order upon the Nb substitution is directly attributed to the reduction in the Fe-O-Mo-O-Fe hybridized metallic chain population.

DOI: 10.1103/PhysRevB.79.035105 PACS number(s): 71.30.+h, 78.70.Dm, 75.47.Gk

I. INTRODUCTION

Since large low-field tunneling type magnetoresistance (MR) at room temperature was found in an ordered double perovskite Sr_2FeMoO_6 (SFMO),[1] iron-based double perovskites such as Sr_2FeMoO_6 and Sr_2FeReO_6 have taken renewed attentions. Their ferrimagnetic Curie temperatures $(T_C \geq 400$ K) are much higher than those of the colossal magnetoresistance (CMR) manganites, and the half-metallic nature was also predicted in the band calculations.[2] The general formula of double perovskites has often been presented as $A_2BB'O_6$, where the B and B' are different transition-metal (TM) ions and located at the center of each perovskite structure as in ABO_3 and $AB'O_3$. The ideal structure consists of alternative arrangements of corner sharing BO_6 and $B'O_6$ octahedrons along the three crystal axes. In the ionic view, the Fe and Mo valence states in SFMO were considered to be $Fe^{3+}(3d^5, S=5/2)$ and $Mo^{5+}(4d^1, S=1/2)$, respectively. Their spins are aligned antiparallel to each other, and the total spin magnetic moment is $4\mu_B$ per formula unit (f.u.). This ionic model, however, is naïve, especially for the Mo 4d states, which are rather itinerant in the metallic SFMO. It was suggested that the Fe local spins are ordered ferromagnetically through the itinerant Mo 4d states strongly hybridized with the Fe 3d states.[3] The band calculation predicted the half-metallic nature that the fully occupied Fe 3d majority-spin bands are separated from the unoccupied Mo 4d majority-spin bands while the minority-spin band with a strong mixture character of the Mo t_{2g} and Fe t_{2g} crosses the Fermi level.[2,4] The x-ray magnetic circular dichroism (XMCD) at Mo $L_{2,3}$ and $M_{2,3}$ edges, the neutron-powder diffraction, and the Mössbauer measurements, which confirmed the Mo 4d spin moment antiparallel to the Fe one, agreed that the Fe state is a mixed valence state closed to $Fe^{2.5+}$ in average.[3,5,6]

Considering the fact that the half-metallic ferromagnetic nature of SFMO is originated from the itinerant 4d electrons, it is an important issue how the physical properties and the electronic structure evolve as the 4d electrons are gradually removed.[7] In this sense, $Sr_2(Fe_{1-z}Mn_z)MoO_6$, in which Fe ions are substituted with the one-electron less Mn ions, has been intensively studied.[8,9] It was found that the system undergoes the metal-insulator transition around $z=0.2$ while the ferromagnetic phase lasts up to $z=0.6$. However, Mn 3d unoccupied states are energetically much higher than the Fe 3d states,[9] and thus, this substitution not only causes the removal of the Mo 4d electrons but also shifts up the 3d state with $S=5/2$ local spin energetically. The more ideal system could be $Sr_2Fe(Mo_{1-x}Nb_x)O_6$, in which the Mo 4d electrons are directly removed by the Nb substitutions, and Sr_2FeNbO_6 (SFNO) becomes an antiferromagnetic or spin-glass-type insulator due to the Nb^{5+} $(4d^0)$ ions without the 4d electrons.[10]

In this paper, we report influences of Nb substitution at Mo sites on the physical properties and electronic structure in $Sr_2Fe(Mo_{1-x}Nb_x)O_6$ $(0 \leq x \leq 1)$. We characterize the crys-

tal structure and magnetic and transport properties. We also investigated the electronic evolution using the soft x-ray absorption spectroscopy (XAS) and XMCD. XAS and XMCD are powerful tools to study the electronic structure and the ferromagnetic characteristics, respectively, especially for the TM compounds since the XAS spectral line shape at the $L_{2,3}$ edge is very sensitive to the ground-state symmetry due to the characteristic multiplet structure.[11] The O K-edge XAS, which utilizes the O $1s \rightarrow 2p$ process, is known to reflect the unoccupied conduction bands in oxides due to the hybridization between the O $2p$ and unoccupied TM $3d/4d$ states.[12] In the study, we found that the substituted Nb ion indeed gets rid of the itinerant Mo $4d$-Fe $3d$ hybridized minority electron to diminish the ferromagnetic characters. When more than two third ($x > 0.7$) of them are removed, the ferromagnetic character disappears as in $Sr_2(Fe_{1-z}Mn_z)MoO_6$. However, the metallic character remains above $x=0.2$ and lasts up to $x=0.6$, different from $Sr_2(Fe_{1-z}Mn_z)MoO_6$. This result indicates that the Fe-O-Mo-O-Fe chain is the essential factor for the half-metallic ferromagnetism in SFMO.

II. EXPERIMENTS

Polycrystalline $Sr_2Fe(Mo_{1-x}Nb_x)O_6$ $(0 \leq x \leq 1)$ samples were grown by the standard solid-state reaction method. $SrCO_3$, Fe_2O_3, MoO_3, and Nb_2O_5 in the desired proportions were mixed and ground in an agate mortar. The mixed powders were decarbonated at 950 °C in an air environment. The decarbonated powders were reground and pressed into disk-shaped pellets, which were calcined in a current flow of 2% H_2/Ar three times for each sample; the first calcination at 950 °C in 5 h, the second one at 1000 °C in 10 h, and the third one at 1050 °C in 12 h. The calcined mixtures, which were ground and pressed into disk-shaped pellets, were sintered in 10 h at 1100 °C in a current flow of 2% H_2/Ar, and then cooled to room temperature at a rate of 20 °C/hour. The phase purity and structural parameters were examined in the x-ray powder-diffraction (XRD) measurement at room temperature by using Rikaku diffractometer with Cu K_α line.

The saturation magnetization was obtained from the M vs H hysteresis curve, which was obtained in an applied field ranging from −8 to 8 T at 5 K by using a commercial magnetic property measurement system (MPMS). The temperature dependence of magnetization (M vs T curve) was measured by using a vibrating sample magnetometer (VSM) at 0.1 T in a temperature range from 5 to 420 K. The temperature dependence of resistivity (ρ vs T) was measured in a temperature range of 5 to 350 K by using a conventional four-probe method. The XAS spectra at Fe $L_{2,3}$, Mo $M_{2,3}$, and O K edges were collected from clean surfaces fractured *in situ* under a vacuum of 1×10^{-9} Torr in a total electron yield (TEY) mode at the 11A Dragon beamline at National Synchrotron Radiation Research Center (NSRRC) in Taiwan. The XMCD measurements were performed at 80 K with 80% circularly polarized incoming light. The XAS measurements were done with 98% linearly polarized light at 200 K to minimize attachment of the water molecules on the surface during the measurement, which especially affect the O K-edge XAS. The magnetization direction in the XMCD

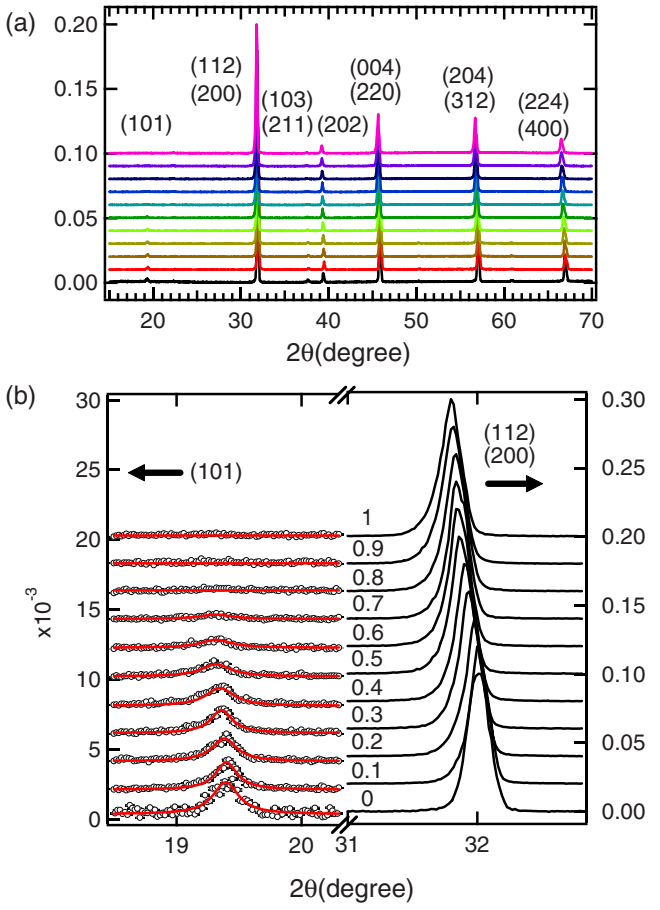

FIG. 1. (Color online) (a) Full profiles of x-ray powder-diffraction patterns of $Sr_2Fe(Mo_{1-x}Nb_x)O_6$ $(0 \leq x \leq 1)$ at room temperature with $I4/mmm$ symmetry index. (b) The (101) peaks, which reflect the degrees of cation ordering, are presented at the left panel. The (112) and (200) peaks are at the right panel.

measurements was aligned parallel and antiparallel to the photon helicity vector by a 0.7 T magnetic field produced by an electromagnet with a maximum field of 1.3 T, and was flipped at each data point during the XMCD measurements. The 0.7 T was found to be large enough to saturate the ferromagnetic signals for all ferromagnetic samples.[13] The XAS and XMCD spectra were normalized by the photon flux monitored with a Au mesh.

III. RESULTS AND DISCUSSION

A. Physical properties

1. Crystal structure

The full profiles of the XRD patterns of $Sr_2Fe(Mo_{1-x}Nb_x)O_6$ $(0 \leq x \leq 1)$ are presented in Fig. 1(a). Rietveld analysis confirms that all the samples are in a single phase with a tetragonal symmetry in a space group $I4/mmm$ without any noticeable hint of impurity phases. The right side of Fig. 1(b) shows the magnified (112) and (200) peak region. As can be seen in the figure, both peak positions shift monotonically to low 2θ angles with increase in the Nb substitution x, confirming the monotonic increases in the lattice

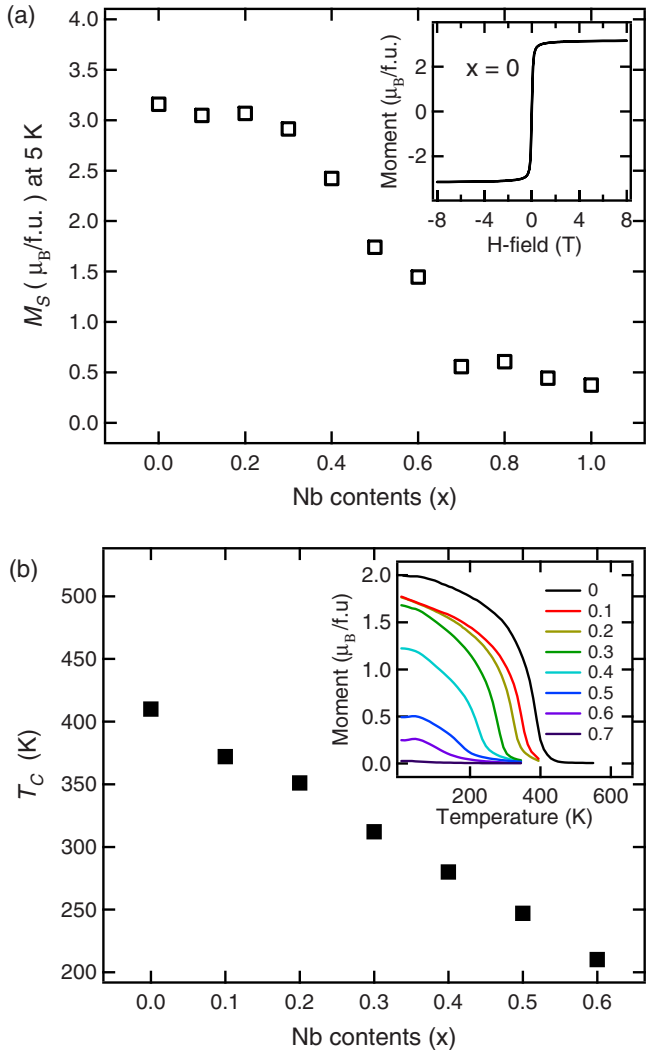

FIG. 2. (Color online) (a) Saturated magnetization M_S for $Sr_2Fe(Mo_{1-x}Nb_x)O_6$. The hysteresis curve of Sr_2FeMoO_6 at 5 K is presented in the inset. (b) Curie temperature T_C for $Sr_2FeMo_{1-x}Nb_xO_6$ measured under a field of 0.1 T after zero-field cooling down to 5 K. M vs T curves for $x \leq 0.7$ are presented in the inset.

parameters and volume. To examine the cation-site (Fe and Mo/Nb) ordering, we checked the (101) superlattice peak, which intensity directly reflects the degree of the site ordering. As can be seen in the left side of Fig. 1(b), the peak intensity gradually decreases as x increases, and it becomes almost negligible for $x > 0.7$. This result indicates that the Nb substitution increases the cation-site disorder, probably due to the very similar ionic size of Fe and Nb.[14] This cation-site disorder, the so-called antisite disorder, is known to disrupt the ferromagnetic order,[1] and consistently reduces the magnetization as discussed below.

2. Magnetic properties

We investigated the magnetic properties of the ferromagnetic double perovskite $Sr_2Fe(Mo_{1-x}Nb_x)O_6$. Figure 2(a) shows the saturated magnetization (M_S) at 5 K at 8 T for different Nb contents x's. The M vs H curve of Sr_2FeMoO_6 ($x=0$) presented in the inset shows that the 8 T is large enough to saturate the magnetization, and the obtained M_S reaches up to $\sim 3.15\mu_B$. This value corresponds to 79% of the expected full moment $4\mu_B$/f.u. for Fe^{3+} ion and Mo^{5+} in the perfect cation order, indicating that the sample has $\sim 10\%$ cation disorders as reported previously.[1] As the Nb substitution x increases, M_S becomes gradually reduced up to $x=0.7$. For $x \geq 0.7$, M_S stays at a very small value, which is expected to be mostly contributed by a paramagnetic background.[15] Indeed, the low-field M-T curves at 0.1 T presented in the inset of Fig. 2(b) shows that the magnetization in the $x=0.7$ is even less than 1% of that in the $x=0$ at 5 K. It is expected that the system for $x \geq 0.7$ is not ferromagnetic in overall. But there possibly exist a very small portion of ferromagnetic local domains with the less Nb content due to the random distribution.

The Curie temperatures T_C's for $x \leq 0.6$ were determined from the M-T curves. As can be seen in Fig. 2(b), T_C monotonically decreases from 412 K for the $x=0$ to 203 K for the $x=0.6$ as x increases. Nb has one less electron than Mo, and thus, the Nb substitution is expected to reduce the number of the itinerant $4d$ electrons contributing the charge carriers. This reduction seems to decrease the ferromagnetic coupling strength and lower T_C as suggested by Navarro *et al.*[16] For $x \geq 0.7$, the loss of the ferromagnetic coupling is so large that the ferromagnetic order may not survive.

The reduction in the coupling strength decreases T_C. However, it is expected to be irrelevant to the local moment, and the ordered moment at low temperature should barely change with the increase in the Nb substitution as long as the system is ferromagnetic. Thus the large reduction in the ordered moment with increase in the x value should be caused by a different origin such as the antisite disorder. As discussed previously,[1] the antisite disorder transforms the Fe-Mo(Nb)-Fe networks into local Fe-Fe and Mo(Nb)-Mo(Nb) pairs, in which the Fe local spins are antiferromagnetically coupled. The low-field magnetization at 5 K is compared with the degree of the antisite ordering determined from the (101) XRD superlattice peak intensity [see Fig. 1(b)] in Fig. 3. Indeed the peak intensity shows very similar x dependence to that of the magnetization, confirming that the reduction in the magnetization is mainly caused by the antisite disorder.

3. Resistivity

The electrical properties of $Sr_2Fe(Mo_{1-x}Nb_x)O_6$ were examined by using the transport measurements. Figure 4 shows the normalized resistivity $[\rho(T)/\rho(300\ \mathrm{K})]$ as a function of temperature for $0 \leq x < 1$. Due to the strong insulating character of SFNO ($x=1$), its resistivity, which is out of the range, is not presented in the same panel. As can be seen in the figure, the normalized resistivity at low temperature greatly increases with increase in x. Even in the metallic SFMO ($x=0$), the resistivity increases upon cooling although its variation is only minimal, indicating that the resistivity is governed by the tunneling and/or diffusion currents through grain boundaries. As x increases, the variation with temperature becomes greatly enhanced, showing that the system become less metallic. Such behaviors can be attributed to the decrease in the charge carriers induced by the Nb substitu-

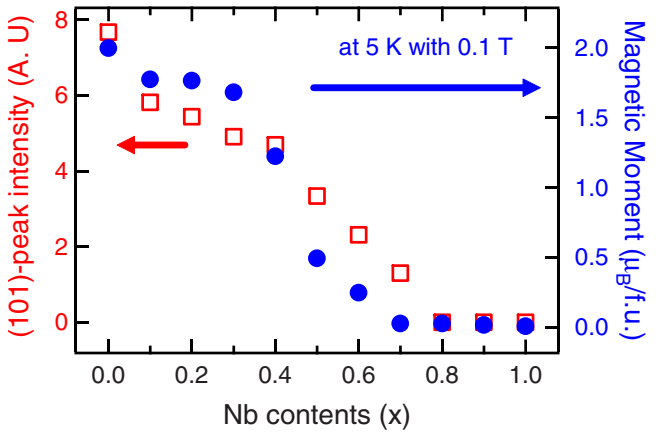

FIG. 3. (Color online) (a) Comparison between the 0.1 T low-field magnetic moments at 5 K (filled circles) and the (101) superlattice peak intensities (open squares) proportional to the degrees of the cation-site ordering.

tion, which reduces the number of itinerant $4d$ electrons. For $x \geq 0.7$, in which the system is not ferromagnetic, we barely observed the metallic Fermi cut-off feature in the valence-band photoemission spectrum and the system is nearly insulating,[17] indicating that the loss of the metallicity accompanies the loss of the ferromagnetism.

B. Electronic evolution

The electronic states of $Sr_2Fe(Mo_{1-x}Nb_x)O_6$ $(0 \leq x \leq 1)$ were investigated by using the XAS at Fe $L_{2,3}$, Mo $M_{2,3}$, and O K edges. The magnetic states were also examined using the XMCD at Fe $L_{2,3}$ edges.

1. XAS at Fe $L_{2,3}$ *edge*

Figure 5(a) presents the Fe $L_{2,3}$-edge XAS spectra. The spectra are normalized to give the same intensity well above the edges. The spectra are generally divided into L_3(706 ~ 716 eV) and L_2(716 ~ 730 eV) regions due to the large Fe $2p$ core-hole spin-orbit coupling energy at the final state.

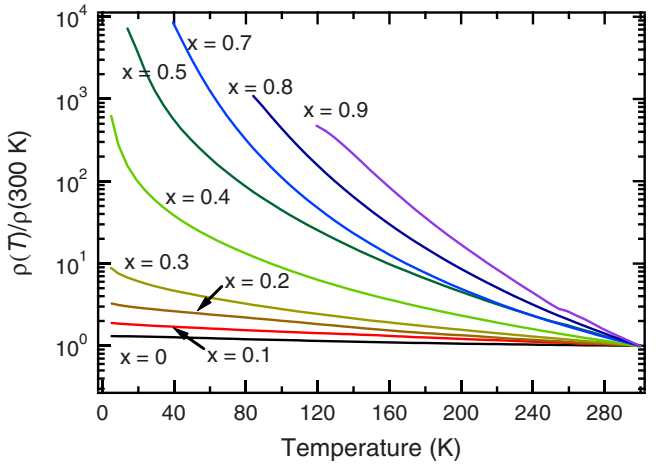

FIG. 4. (Color online) Temperature dependence of normalized resistivity for $Sr_2Fe(Mo_{1-x}Nb_x)O_6$ $(0 \leq x \leq 0.9)$.

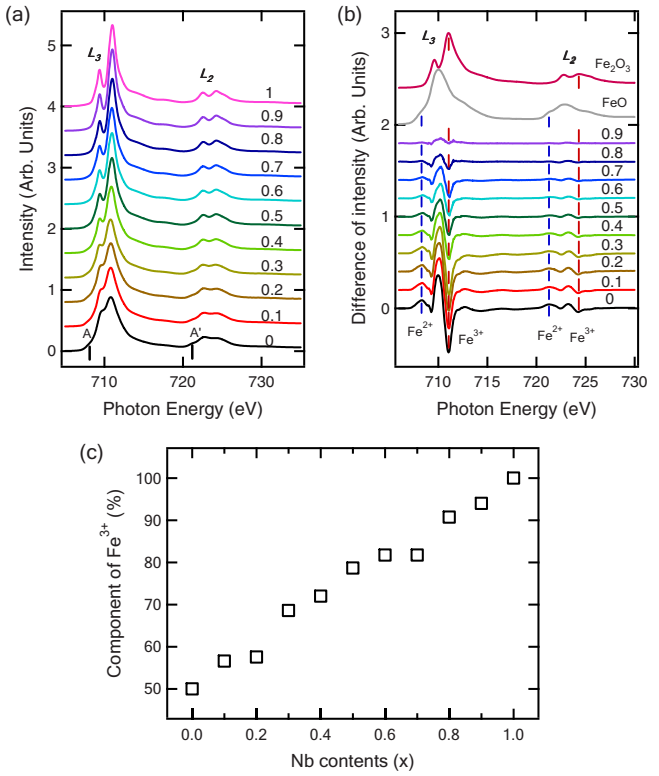

FIG. 5. (Color online) (a) Fe $L_{2,3}$-edge XAS spectra of $Sr_2Fe(Mo_{1-x}Nb_x)O_6$ $(0 \leq x \leq 1)$ measured at 200 K. The spectra were normalized to have the same intensity well above the edge. (b) Difference spectra obtained by subtracting the SFNO spectrum from corresponding ones. The spectra of FeO and Fe_2O_3 are taken from Ref. 21. (c) The compositions of Fe^{3+} determined from the difference spectra under the assumption of the compositions in the two end members, 50% in SFMO (x=0) and 100% in SFNO (x =1.0)

As x increases, the overall spectral weight in both regions shifts into high photon energy and the spectral line shape changes gradually. These behaviors obviously reflect the Fe valence change: (1) The spectral weight shift, the so-called chemical shift, to high-energy means that the Fe valence increases. (2) The spectral line shape represents the characteristic multiplet structure of the initial state, and thus, its change is considered as a natural result of the valence change. The spectrum of SFMO (x=0), which agrees with that in the previous reports, is well explained in terms of an Fe^{2+}-Fe^{3+} mixed-valence state with an average valence close to $Fe^{2.5+}$.[18,19] In comparison with that of SFNO (x=1.0), which displays the typical multiplet structure of the Fe^{3+} monovalence state as in α-Fe_2O_3,[20] the line shape agrees with that of SFMO at the high-energy side in each region, while it presents an extra pre-edge feature at the low-energy side [denoted by A and A' in Fig. 5(a)], which is also observable in the spectrum of the divalent iron oxide (Fe^{2+}) like FeO.[21] The spectral changes for $0.0 \leq x \leq 1.0$ tell us that the average Fe valence gradually varies from ~+2.5 for x=0 to +3 for x=1.

The more clear and quantitative characterization for Fe^{2+} and Fe^{3+} contributions can be made by subtracting the SFNO Fe^{3+} spectrum from the others. The difference spectra are

compared with those of reference materials FeO and α-Fe_2O_3 in Fig. 5(b). The Fe^{2+} and Fe^{3+} contributions can be identified as follows: (1) The larger positive and negative values in intensity represent the more Fe^{2+} and Fe^{3+} states, respectively. (2) The intensities of the positive peak and negative deep are proportional to the Fe^{2+} and Fe^{3+} compositions, respectively. The estimated compositions from the corresponding intensities under assumption of the average iron valence $Fe^{2.5+}$ for SFMO and Fe^{3+} for SFNO are presented in Fig. 5(c). One can recognize that the average valence well agrees with the amount of Nb (x). The Fe^{2+} (Fe^{3+}) composition almost linearly decreases (increases) with x. Apparent small deviations from the linear behavior are expected to be come from deviations in the oxygen stoichiometry. Considering that the Nb substitution disrupts the Fe-O-Mo connection and its population deceases by the amount of the substitution x, this result indicates that the Fe mixed-valence state is caused by the strong hybridization between Fe $3d$ and Mo $4d$ states in the Fe-O-Mo connection.

2. XMCD at Fe $L_{2,3}$ edge

Figure 6(a) shows the Fe $L_{2,3}$-edge XMCD results of $Sr_2Fe(Mo_{1-x}Nb_x)O_6$ ($0 \leq x \leq 0.6$) measured at 80 K. The left panel shows the XAS spectra for photon helicities parallel ($\rho+$) and antiparallel ($\rho-$) to the magnetization direction (Fe $3d$ majority-spin direction). The difference spectra ($\Delta\rho = \rho_+ - \rho_-$) and their integrals [$\Sigma(\Delta\rho)$] are presented in the right panel. As the Nb amount x increases, the difference signal ($\Delta\rho$) becomes weaker, showing that the ferromagnetically ordered net spin moment gets smaller, consistent with the magnetization data presented in Fig. 2. On the other hand, the integration over the entire spectral range, which is proportional to the orbital magnetic moment, is almost negligible for all measured samples, showing that the orbital magnetic moment of Fe $3d$ states is nearly quenched. The t_{2g} orbital state effectively corresponds to the angular-momentum $L=1$ state. Thus the minority-spin t_{2g} electron would contribute a considerable orbital magnetic moment if the state were localized.[22] The vanishing orbital moment indicates that the down-spin t_{2g} state is very itinerant. It is also consistent with that the Fe^{2+} in these double perovskites is induced by its strong hybridization with the itinerant down-spin Mo t_{2g} state near E_F. For $x \geq 0.7$, the XMCD does not show any considerable magnetic circular dichroism (MCD) signal at the given magnetic field ($H=0.7$ T), which is large enough to saturate the ferromagnetic signal for the $x=0.6$ sample.[13] This indicates that the ferromagnetic long-range ordering does not retain at 80 K. Considering that $T_C \simeq 210$ K for the $x=0.6$ sample, one can conclude that the system with $x \geq 0.7$ is not in the intrinsic ferromagnetic phase.

Figure 6(b) shows the magnetic moments estimated from the XMCD results by using the sum rule[23] in comparison with the low-field moments at 80 K obtained from the M-T curves presented in Fig. 2(b). The estimated moments show very similar behavior to the low-field ones, which are somewhat smaller values than those obtained from SQUID at 5 K and 8 T presented in Fig. 2(a). Considering that the estimated moments reflect only the Fe $3d$ moment and that the measurements were performed at 80 K and 0.7 T, at which the paramagnetic background contribution becomes negligible, the obtained moments are very consistent with the SQUID results. The estimated moment from the XMCD sum rule corresponds to the net ferromagnetic moment, and thus, the reduction in the moment with the increase in x reflects the increase in the antisite disorder, which contributes antiparallel alignments of the Fe spins, as discussed above.

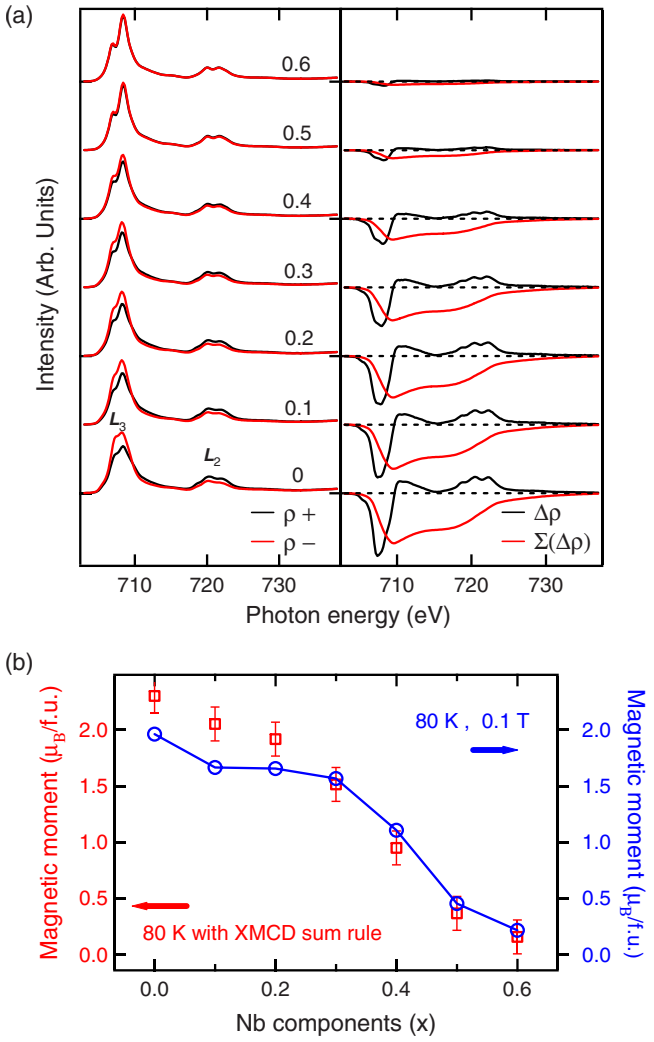

FIG. 6. (Color online) (a) Fe $L_{2,3}$-edge XMCD results for $Sr_2Fe(Mo_{1-x}Nb_x)O_6$ ($0 \leq x \leq 0.6$) at 80 K. The left panel shows the XAS spectra for different photon helicities, and the difference spectra and their integrals are presented in the right panel. (b) Magnetic moments at the Fe site estimated from XMCD compared with those determined from the low-field M-T curves at 80 K presented in Fig. 2(b).

3. XAS at Mo $M_{2,3}$ edge

Now we examine how the Nb substitution affects the Mo valence state. Figure 7 presents the Mo $M_{2,3}$-edge ($3p_{1/2,3/2} \rightarrow 4d$) XAS spectra for the series of $Sr_2Fe(Mo_{1-x}Nb_x)O_6$ ($0 \leq x \leq 0.9$).[24] The spectra are generally divided into Mo M_3 and M_2 regions at low and high photon energies due to the large Mo $3p$ core-hole spin-orbit coupling energy. The spec-

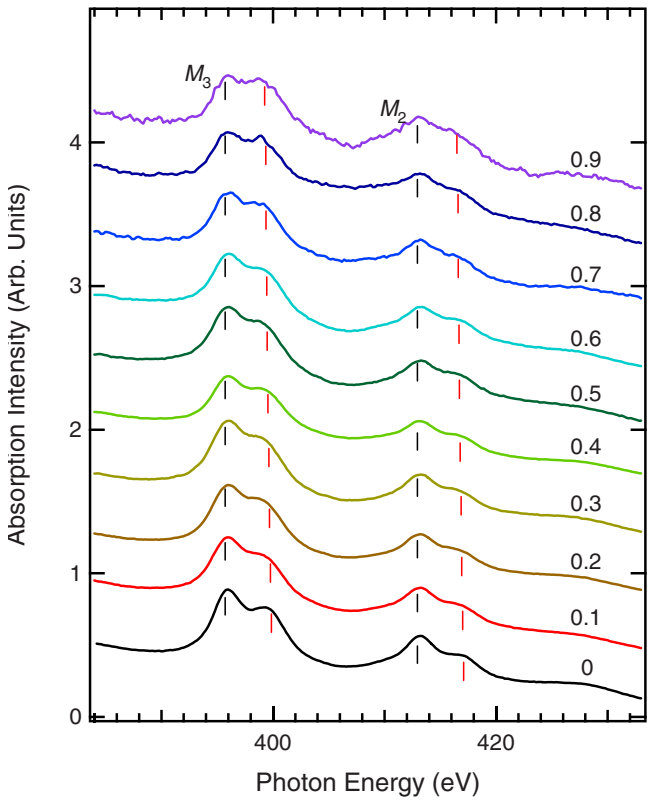

FIG. 7. (Color online) Mo $M_{2,3}$-edge XAS spectra of $Sr_2Fe(Mo_{1-x}Nb_x)O_6$ $(0 \leq x \leq 1)$ measured at 200 K.

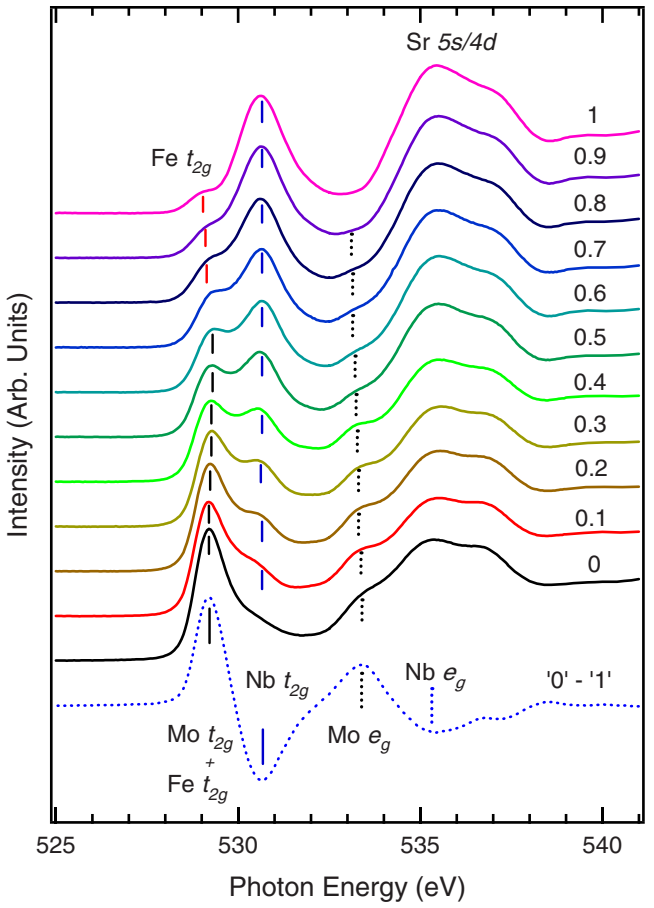

FIG. 8. (Color online) Oxygen K-edge XAS spectra of $Sr_2Fe(Mo_{1-x}Nb_x)O_6$ $(0 \leq x \leq 1)$ measured at 200 K. The difference spectrum (dashed line) is obtained by subtracting the SFNO ($x=1$) spectrum from the SFMO ($x=0$) one.

tral line shape at both regions is dominated by two main features. Due to the spatially extended character of the Mo 4*d* states, the atomic multiplet effects are minimized. Thus the spectra simply display the unoccupied Mo 4*d* states and these two features can be interpreted as the unoccupied Mo t_{2g} and e_g bands at low and high energies, respectively. Therefore the relative spectral weight of these two features directly provides the Mo valence state since the Mo 4*d* electrons only occupy the low-lying t_{2g} band. The Nb substitution, however, barely affects the relative weight, the change is even less than the estimation error (<5%) for all the samples, indicating almost no change in the Mo valence. Although the relative weight stays at nearly constant within the estimation error, the spectrum still shows small but certain gradual changes in the spectral line shape as x increases. These changes are due to gradual reduction in the energy separation between the t_{2g} and e_g bands, which corresponds to the octahedral crystal-field splitting energy 10Dq. The 10Dq value estimated from the spectra turns out to be reduced from 4.2 ± 0.2 eV for $x=0.0$ to 3.8 ± 0.2 eV for $x=0.9$. These values coincide with those estimated from the O K-edge XAS spectra for the different x's discussed below. As discussed above, the Nb substitution diminishes the metallic character. The XRD results [see Fig. 1(b)] show that the lattice parameters and unit-cell volume slightly increase with the Nb substitution, which also bring with the loss of the metallicity. The Mo-O interatomic distance seems to increase with the loss of the metallicity, and the reduction in the 10Dq value can be attributed to the reduced Mo 4*d*-O 2*p* local hybridization strengths.

4. XAS at O K edge

Figure 8 shows the O K-edge XAS spectra of $Sr_2Fe(Mo_{1-x}Nb_x)O_6$ $(0 \leq x \leq 1)$. These spectra correspond to the O 2*p* partial density of states due to the hybridization between the unoccupied states and the O 2*p* state, and thus can be considered as the weighted electronic structure of the conduction band. The spectra were normalized to have the same intensity well above the absorption threshold (~570 eV). The spectra are generally divided into two regions, Mo 4*d*/Nb 4*d*/Fe 3*d* states and Sr 4*d*, 5*s*/Mo 5*s*/Nb 5*s*/Fe 4*s* states at low and high energies, respectively. Here we only focus on the low-energy region states, which determine the physical properties of these compounds. Indeed, the spectral line shape in this region greatly varies with the amount of the Nb substitution. Since the hybridization strength of the Mo/Nb 4*d* states is much larger than that of the Fe 3*d* states, the spectral weight is dominated by the Mo/Nb 4*d* states.

The spectrum of SFMO ($x=0$), which agrees with the reported one,[9] shows a high intensity peak near the threshold (~529 eV) and a wide bump feature around 533 eV. The respective two states correspond to the Mo 4*d* t_{2g} and e_g bands, which are separated by the large crystal-field energy 10Dq ~ 4 eV. This 10Dq value is in a good agreement with

previously reported one in the optical result[9] and also in the band theory.[1,25] On the other hand, the spectrum of SFNO ($x=1$) shows a high intensity peak at ~531 eV, which corresponds to Nb 4d t_{2g} band, but the e_g band cannot be identified in the spectrum. Its 10Dq value is supposed to be similar to that of SFMO, and the e_g band peak is expected to be overlapped with the broad high energy Sr 4d,5s/Mo 5s/Nb 5s/Fe 4s states.

The more clear identification can be made in the difference spectrum, which is also presented in the figure. The difference spectrum was obtained by subtracting the SFNO ($x=1$) spectrum from the SFMO ($x=0$) one. The positive peaks at ~529 eV and ~533 eV result from the Mo t_{2g} and e_g bands, while the negative peaks at ~531 eV and ~536 eV from Nb t_{2g} and e_g bands, respectively. The 10Dq value of Nb 4d was estimated to be 4.6 ± 0.2 eV, which is somewhat larger than that of Mo 4d. This about 10% enhancement in 10Dq is consistent with the smaller Nb-O distance and is also observed in $SrMO_3$ (M=4d transition metals) series.[26] As seen in the Mo $M_{2,3}$-edge XAS study discussed above, we also found that the 10Dq value of the Mo 4d states becomes slightly reduced as x increases, from $10Dq=4.2\pm0.2$ eV for the $x=0$ to 3.8 ± 0.2 eV for $x=0.9$. In the spectrum of SFNO, besides the Nb 4d bands, a small bump shows up at ~529 eV, which corresponds to the Fe t_{2g} band. From the previous study on $Sr_2Fe_{1-x}Mn_xO_6$,[9] we identified that the Fe t_{2g} band in Sr_2FeMoO_6 ($x=0$) locates at ~529.5 eV, i.e., ~0.5 eV energy shift, which is probably due to the different Fe 3d bond environments with Mo 4d and Nb 4d.

5. Electronic structure in the conduction bands

The electronic structure in the conduction bands for Sr_2FeMoO_6 and Sr_2FeNbO_6 can be summarized by the schematic energy diagrams presented in Fig. 9. The Fe t_{2g} (down spin) band energetically locates very close to the Mo t_{2g} band, which locates near E_F. Hence the down-spin Fe t_{2g} states are expected to strongly hybridized with the down-spin Mo t_{2g} states in the Fe-O-Mo local connections. The charge carriers have strong mixture characters of Fe and Mo t_{2g} states, resulting in the Fe^{2+}-Fe^{3+} mixed-valence state and the average valence close to $Fe^{2.5+}$. On the other hand, the energy locations of Nb 4d bands, both t_{2g} and e_g, shift up by about 2 eV in comparison with those of Mo 4d bands. This energy shift makes the Nb t_{2g} band well separated from the Fe t_{2g} band. Hence the Nb substitution replaces the Fe-O-Mo local connection with the Fe-O-Nb one and reduces the charge carriers near E_F with the strong mixture character of Fe t_{2g}-Mo t_{2g} down-spin states. The loss of the Fe-O-Mo local connection transforms the mixed-valence state into the Fe^{3+} monovalent state.

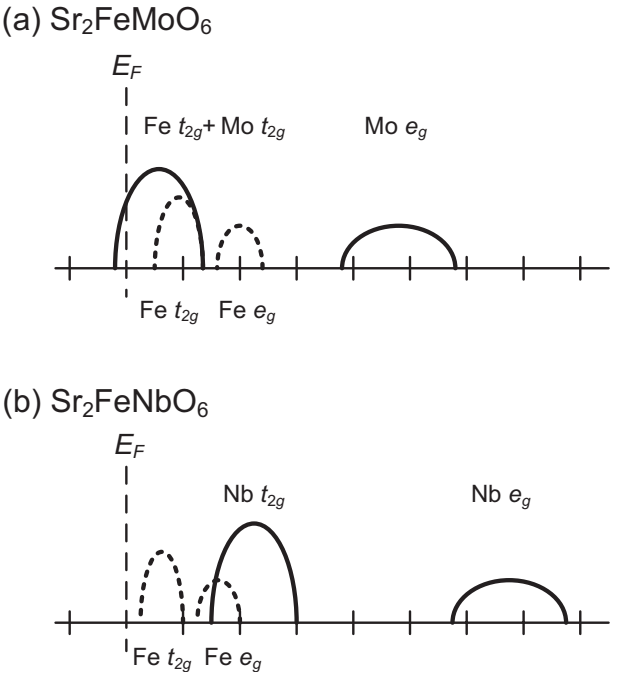

FIG. 9. Schematic energy diagrams of unoccupied conduction bands for (a) Sr_2FeMoO_6 and (b) Sr_2FeNbO_6.

IV. SUMMARY AND CONCLUSIONS

We systematically investigated the physical properties of $Sr_2(FeMo_{1-x}Nb_x)O_6$ ($0\le x\le 1$) and the electronic evolution as a function of the Nb substitution. For all the range of the Nb substitution, $0\le x\le 1$, XRD showed that all the samples are in a single phase with a tetragonal symmetry and the lattice parameters monotonically increase with increase in x. The degree of the antisite disorder increases with the Nb substitution due to the very similar ionic sizes of Fe and Nb, and the degree of the Fe-Mo/Nb cation-site ordering becomes negligible for $x>0.7$. In the magnetic properties, the low-temperature ordered magnetic moment greatly decreases, as also confirmed in the XMCD measurements, and T_C becomes lowered as x increases. The lowering of T_C should be attributed to the weakened intersite ferromagnetic coupling due to the reduction in the population of the Fe 3d-O 2p-Mo 4d connections and also the reduction in the charge carriers. For $x\ge 0.7$, the loss of the Fe-O-Mo connections becomes so large that the system becomes nearly insulating, i.e., almost no charge carriers, and the ferromagnetic ordering disappears. On the other hand, the reduction in the ordered magnetic moment is mainly caused by the antisite disorder. Indeed the low-temperature ordered moment shows very similar x dependence to that of the degree of the cation-site ordering.

The electronic evolution induced by the Nb substitution, which reduces the Fe-O-Mo connections, was investigated by using the XAS at Fe $L_{2,3}$, Mo $M_{2,3}$, and O K edges. The average valence monotonically changes from $Fe^{2.5+}$ for $x=0$ to Fe^{3+} for $x=1$. On the other hand, the Mo valence is nearly independent of the Nb substitution. The Fe-O-Mo local connections provide the Fe t_{2g}-Mo t_{2g} strongly mixed states resulting in the Fe mixed-valence states. The Mo 4d crystal-field splitting energy 10Dq was estimated to be 4.2 ± 0.2 eV for SFMO ($x=0$). As x increases, it becomes gradually reduced to be 3.8 ± 0.2 eV for $x=0.9$, indicating that the volume expansion and the reductions in the Mo 3d-O 2p hybridization strengths are accompanied with the loss of the metallicity. In comparison with Mo 4d bands, both Nb t_{2g} and e_g bands shift up by about 2 eV so

that the Nb t_{2g} band locates well above E_F and the Nb substitution reduces the number of charge carriers. The 10Dq of the Nb $4d$ bands is estimated to be 4.6 ± 0.2 eV in SFNO ($x=1$). Consequently, the evolution of the electronic structure well explains the physical properties of $Sr_2(FeMo_{1-x}Nb_x)O_6$.

ACKNOWLEDGMENTS

This work was supported by KOSEF under Grant No. R01-2007-000-11188-0, eSSC at POSTECH, POSTECH research fund, and the BK21 program.

*Correspondence should be addressed to jhp@postech.ac.kr

[1] K.-I. Kobayashi, T. Kimura, H. Sawada, K. Terakura, and Y. Tokura, Nature (London) **395**, 677 (1998).

[2] K.-I. Kobayashi, T. Kimura, Y. Tomioka, H. Sawada, K. Terakura, and Y. Tokura, Phys. Rev. B **59**, 11159 (1999).

[3] O. Chmaissem, R. Kruk, B. Dabrouwski, D. E. Brown, X. Xiong, S. Kolesnik, J. D. Jorgensen, and C. W. Kimball, Phys. Rev. B **62**, 14197 (2000).

[4] I. V. Solovyev, Phys. Rev. B **65**, 144446 (2002).

[5] M. Besse, V. Cros, A. Barthélémy, H. Jaffrès, J. Vogel, F. Petroff, A. Mirone, A. Tagliaferri, P. Bencok, P. Decorse, P. Berthet, Z. Szotek, W. M. Temmerman, S. S. Dhesi, N. B. Brookes, A. Rogalev, and A. Fert, Europhys. Lett. **60**, 608 (2002).

[6] J. Lindén, Y. Yamamoti, M. Karppinen, H. Yamauchi, and T. Pietari, Appl. Phys. Lett. **76**, 2925 (2000).

[7] J. L. Alonso, L. A. Fernández, F. Guinea, F. Lesmes, and V. Martín-Mayor, Phys. Rev. B **67**, 214423 (2003).

[8] Y. Moritomo, H. Kusuya, A. Machida, E. Nishibori, M. Takata, M. Sakata, and A. Nakamura, J. Phys. Soc. Jpn. **70**, 3182 (2001).

[9] J. H. Jung, S.-J. Oh, M. W. Kim, T. W. Noh, J.-Y. Kim, J.-H. Park, H.-J. Lin, C. T. Chen, and Y. Moritomo, Phys. Rev. B **66**, 104415 (2002).

[10] R. Rodríguez, A. Ferández, A. Isalqué, J. Rodríguez, A. Labarta, J. Tejada, and X. Obradors, J. Phys. C **18**, L401 (1985).

[11] F. M. F. de Groot, J. C. Fuggle, B. T. Thole, and G. A. Sawatzky, Phys. Rev. B **42**, 5459 (1990); J.-H. Park, C. T. Chen, S.-W. Cheong, W. Bao, G. Meigs, V. Chakarian, and Y. U. Idzerda, Phys. Rev. Lett. **76**, 4215 (1996).

[12] F. M. F. de Groot, M. Grioni, J. C. Fuggle, J. Ghijsen, G. A. Sawatzky, and H. Petersen, Phys. Rev. B **40**, 5715 (1989); D.-Y. Cho, J.-Y. Kim, B.-G. Park, K.-J. Rho, J.-H. Park, H.-J. Noh, B. J. Kim, S.-J. Oh, H.-M. Park, J.-S. Ahn, H. Ishibashi, S.-W. Cheong, J. H. Lee, P. Murugavel, T. W. Noh, A. Tanaka, and T. Jo, Phys. Rev. Lett. **98**, 217601 (2007).

[13] Before the XMCD measurement on each sample, the saturation field was examined in the magnetic hysteresis curve obtained by monitoring the flourescence yield signal at the Fe L_2 white line in the external field scan.

[14] The average intersite distance in the $Nb^{5+}O_6^{2-}$ octahedron is 2.04 Å, which is nearly identical to that in the $Fe^{3+}O_6^{2-}$ one (2.045 Å); see R. D. Shannon and C. T. Prewitt, Acta Crystallogr. B **25**, 925 (1969).

[15] The Zeeman splitting at 8 T is expected to be large enough to partially overcome the thermal energy at 5 K.

[16] J. Navarro and C. Frontera, LI. Balcells, B. Martínez, and J. Fontcuberta, Phys. Rev. B **64**, 092411 (2001).

[17] B.-G. Park *et al.* (unpublished).

[18] D. D. Sarma, P. Mahadevan, T. Saha-Dasgupta, Sugata Ray, and Ashwani Kumar, Phys. Rev. Lett. **85**, 2549 (2000).

[19] J.-S. Kang, J. H. Kim, A. Sekiyama, S. Kasai, S. Suga, S. W. Han, K. H. Kim, T. Muro, Y. Saitoh, C. Hwang, C. G. Olson, B. J. Park, B. W. Lee, J. H. Shim, J. H. Park, and B. I. Min, Phys. Rev. B **66**, 113105 (2002).

[20] J.-Y. Kim, T. Y. Koo, and J.-H. Park, Phys. Rev. Lett. **96**, 047205 (2006).

[21] J.-H. Park, Ph. D. thesis, The University of Michigan, 1994.

[22] D. J. Huang, C. F. Chang, H.-T. Jeng, G. Y. Guo, H.-J. Lin, W. B. Wu, H. C. Ku, A. Fujimori, Y. Takahashi, and C. T. Chen, Phys. Rev. Lett. **93**, 077204 (2004).

[23] C. T. Chen, Y. U. Idzerda, H.-J. Lin, N. V. Smith, G. Meigs, E. Chaban, G. H. Ho, E. Pellegrin, and F. Sette, Phys. Rev. Lett. **75**, 152 (1995).

[24] The spectra were obtained after subtraction of Nb $M_{2,3}$-edge XAS background signal, which affects the downhill slope in the Mo $M_{2,3}$-edge XAS spectrum region.

[25] H.-T. Jeng and G. Y. Guo, Phys. Rev. B **67**, 094438 (2003).

[26] Y. S. Lee, J. S. Lee, T. W. Noh, D. Y. Byun, K. S. Yoo, K. Yamaura, and E. Takayama-Muromachi, Phys. Rev. B **67**, 113101 (2003); H.-J. Noh, B. J. Kim, S.-J. Oh, J.-H. Park, H.-J. Lin, C. T. Chen, Y. S. Lee, K. Yamaura, and E. Takayama-Muromachi, J. Phys.: Condens. Matter **20**, 485208 (2008).